Eur. Phys. J. B **42**, 157–163 (2004)
DOI: 10.1140/epjb/e2004-00367-6

THE EUROPEAN PHYSICAL JOURNAL B

Dynamics of polaron in a polymer chain with impurities

Y.H. Yan, Z. An, and C.Q. Wu[a]

Research Center for Theoretical Physics, Fudan University, Shanghai 200433, P.R. China

Received 4 June 2004
Published online 14 December 2004 –

Abstract. In a polymer chain, an extra electron or hole distorts the chain to form a charged polaron, which is the charge carrier being responsible for conductivity. When an intermediate-strength electric field is applied, the polaron will be accelerated for a short time and then move at a constant velocity. The dynamical process of polaron in a polymer chain with impurities is simulated within a non-adiabatic evolution method, in which the electron wave function is described by the time-dependent Schrödinger equation while the polymer lattice is treated classically by a Newtonian equation of motion. We have considered two kinds of dynamical processes, one is the field-induced depinning of a charged polaron, which is initially bound by an attractive impurity; and the other is the scattering of a polaron from an impurity. In the former process, the charged polaron will depart from the attractive impurity only for the applied field with strength over a threshold, otherwise, the polaron will oscillate around the impurity. In the latter process, the charged polaron moves through the impurity in the presence of an electric field while it will be bounced back for a repulsive impurity or trapped to oscillate around an attractive impurity in the case that the applied electric field is weak and just be present for the polaron acceleration.

PACS. 71.38.-k Polarons and electron-phonon interactions – 72.80.Le Polymers; organic compounds (including organic semiconductors)

1 Introduction

In recent years, organic electronic devices, e.g., light-emitting diodes and field-effect transistors, are attracting considerable interest because they have processing and performance advantages for low-cost and large-area applications [1]. In these devices, organic polymers are used as the light-emitting and charge-transporting layers, in which the electron and/or hole are injected from the metal electrodes and transported under the influence of an external electric field. Due to the strong electron-lattice interactions, it is well known that additional electrons or holes in conjugated polymers will induce self-localized excitations, such as solitons [2] (only in *trans*-polyacetylene) and polarons [3]. As a result, it has been generally accepted that the charge carriers in conjugated polymers are these excitations including both charge and lattice distortion [4].

There have been extensive studies on soliton and polaron dynamics in conjugated polymers [5–10] under the influence of external electric fields. It is shown that solitons as well as polarons keep their shape while moving along a chain. Solitons are shown to have a maximum velocity $2.7v_s$, where v_s is the sound velocity [6,11]. The situation will be different for polarons, which has been shown to be not created in electric fields over 6×10^4 V/cm due to the charge moving faster and not allowing the distortion to occur [7]. A recent study by Johansson and Stafström [8] deals with the polaron migration between neighboring polymer chains. The numerical results show that the polaron becomes totally delocalized, either before or after the chain jump for the electric field over 3×10^5 V/cm. However, a preexisted polaron in a single chain can survive under the field up to 10^6 V/cm [9,12].

While the stability of polaron motion under the influence of an external electric field has been discussed, we investigate the dynamics of polaron in a polymer chain with impurities in this paper. Electric field induced depinning of a charged soliton from an impurity center in polyacetylene has been considered by Terai and Ono [13]. It should be much more interesting for the polaron dynamics than that of solitons since the latter is only appeared in the degenerate polymers, such as *trans*-polyacetylene. Recently, the motion of polarons (as well as bipolarons) under the influence of an electric field through a single-site impurity was also discussed by considering the impurity molecules functioning as logical switches [14]. In this paper, two kinds of impurities are considered, one is a single-site impurity and the other is a multi-site impurity. With an attractive impurity, the charged polaron will be bound around the impurity. Both of the depinning and scattering processes are simulated within a non-adiabatic dynamical evolution method, in which the electron wave function is described by the time-dependent Schrödinger

[a] e-mail: cqw@fudan.edu.cn

equation while the lattice is treated classically by a Newtonian equation of motion.

The paper is organized as follows. In the following section, we present a tight-binding one-dimensional model for a polymer chain with impurities in an external electric field and then describe the non-adiabatic dynamical evolution method. The polaron configuration and its energies in the presence of an impurity are given in Section 3. The depinning and scattering processes of the charged polaron from an impurity are presented in Sections 4 and 5, respectively, and the summary of this paper is given in Section 6.

2 Model and method

We consider a tight-binding one-dimensional model for a polymer chain that contains an impurity in an external filed. The Hamiltonian consists of three parts,

$$H = H_e + H_{latt} + H_{\rm im}. \tag{1}$$

The electronic part is

$$H_e = -\sum_n t_n \left[e^{-i\gamma A(t)} c_{n+1}^\dagger c_n + \text{h.c.} \right], \tag{2}$$

where $c_n^\dagger$ (c_n) creates (annihilates) an electron at site n, $t_n = t_0 - \alpha(u_{n+1} - u_n)$ is the hopping integral [2] between sites n and $n+1$, α describes the electron-lattice coupling between neighboring sites due to the lattice bond stretch, and u_n is the monomer displacement of site n. The vector potential $A(t)$ is introduced to describe a uniform external electric field along the chain at the periodic boundary condition, the relation between the potential $A(t)$ and the uniform electric field $E(t)$ is given as $E(t) = -(1/c)\partial A(t)/\partial t$, $\gamma \equiv ea/\hbar c$ is a constant quantity, c is the light speed, e the absolute value of the electronic charge, and a the lattice constant. The polymer lattice is described by

$$H_{latt} = \frac{K}{2}\sum_n (u_{n+1} - u_n)^2 + \frac{M}{2}\sum_n \dot{u}_n^2, \tag{3}$$

where K is the elastic constant and M the mass of a CH group [2]. The model parameters we use in this work are those generally chosen for *trans*-polyacetylene [2,4]: $t_0 = 2.5$ eV, $\alpha = 4.1$ eV/Å, $K = 21$ eV/Å^2, $M = 1394.14$ eV fs^2/Å^2, and $a = 1.22$ Å. The impurity is described by

$$H_{\rm im} = \sum_n V_n c_n^\dagger c_n, \tag{4}$$

where V_n is the strength of impurity potential at the nth site. For negative charged polaron, the impurity is attractive for $V_n < 0$ while it is repulsive for $V_n > 0$. Two kinds of impurities are considered in this work: one is a single-site impurity; the other is a multi-site impurity.

In the absence of an external electric field, we can determine the static structure by the minimization of the system energy. First, we can write down the electron eigenequation for a given lattice configuration ($\{u_n\}$) as

$$\epsilon_\mu \phi_\mu(n) = -t_n\phi_\mu(n+1) - t_{n-1}\phi_\mu(n-1) + V_n\phi_\mu(n), \tag{5}$$

from which we can obtain all electron wave functions ($\{\phi_\mu(n)\}$) and then the static energy of the system

$$E_t = -\sum_n t_n(\rho_{n,n+1} + \rho_{n+1,n}) + \frac{K}{2}\sum_n (u_{n+1} - u_n)^2, \tag{6}$$

here, $\rho_{n,n'}$ is the element of density matrix, which will be defined below. The lattice configuration ($\{u_n\}$) is determined by $\partial E_t/\partial u_n = 0$, which gives the self-consistent iteration equations

$$u_{n+1} - u_n = -\frac{\alpha}{K}(\rho_{n,n+1} + \rho_{n+1,n}) + \lambda, \tag{7}$$

where λ is a Lagrangian multiplier to guarantee that the polymer chain with the periodic boundary condition will not collapsed, that is, the chain length will not changed [$\sum_n (u_{n+1} - u_n) = 0$].

Once an electric field is applied along the polymer chain, the initial lattice configuration and the electron distribution determined by the self-consistent iteration equations (5) and (7) will not be kept. The lattice configuration at any time t (> 0) should be governed by the Newtonian equation of motion,

$$M\ddot{u}_n = F_n(t), \tag{8}$$

where the force acting on the nth site consists of two parts, one is the spring force from the bond stretch or compression and the other is the force from the electron-lattice interaction that could be obtained within the Hellmenn-Feynman theorem,

$$F_n(t) = -K(2u_n - u_{n+1} - u_{n-1}) + \alpha\left[e^{i\gamma A(t)}(\rho_{n,n+1} - \rho_{n-1,n}) + \text{c.c.} \right], \tag{9}$$

here, the element of the density matrix is defined as

$$\rho_{n,m}(t) = \sum_k \Psi_k^*(n,t) f_k \Psi_k(m,t), \tag{10}$$

f_k is the time-independent distribution function determined by initial occupation (being 0,1 or 2). The evolution of the electronic wave function $\Psi_k(n,t)$ is determined by the time-dependent Schrödinger equation

$$i\hbar\dot{\Psi}_k(n,t) = -t_n e^{-i\gamma A(t)}\Psi_k(n+1,t) - t_{n-1}e^{i\gamma A(t)}\Psi_k(n-1,t) + V_n\Psi_k(n,t). \tag{11}$$

The numerical integration of equation (8) is quite straightforward. We discretize the time variable, and express the discretized time as t_j and the time interval as Δt. The displacement $u_n(t_{j+1})$ and the velocity $\dot{u}_n(t_{j+1})$ of the nth site at next time $t_{j+1} \equiv t_j + \Delta t$ can be written as

$$u_n(t_{j+1}) = u_n(t_j) + \dot{u}_n(t_j)\Delta t, \tag{12}$$

and

$$\dot{u}_n(t_{j+1}) = \dot{u}_n(t_j) + \frac{1}{M}F_n(t_j)\Delta t \tag{13}$$

respectively. It is clear from this treatment that Δt should be small enough compared to the characteristic time of the lattice vibration (i.e., $\Delta t \ll \omega_Q^{-1}$, here $\omega_Q \equiv \sqrt{4K/M}$ is the bare optical phonon frequency).

Because the electronic wave functions $\Psi_k(t)$'s are not eigenfunctions, the numerical integration of equation (11) is not so straightforward and has to be handled more delicately. If the single particle Hamiltonian operator at time t is expressed as $\hat{h}(t)$, then the solution of the time dependent Shrödinger equation can be written schematically as

$$\Psi_k(t) = \hat{T}\exp\left[-\frac{i}{\hbar}\int_0^t dt'\hat{h}(t')\right]\Psi_k(0), \tag{14}$$

where $\hat{T}$ represents the time ordering operator. If we discretize time and choose the interval Δt small enough, so that $\hat{h}(t)$ changes slightly during Δt, i.e., we can treat $\hat{h}(t)$ as a constant during the time period from t_j to t_{j+1}. Then the above equation can be rewritten as follow,

$$\Psi_k(t_{j+1}) = \exp\left[-i\hat{h}(t_j)\Delta t/\hbar\right]\Psi_k(t_j). \tag{15}$$

In order to solve equation (15), we choose the instantaneous eigenfunctions $\{\phi_\nu\}$ of $\hat{h}(t_j)$ as basis set and expand $\Psi_k(t_j)$ in terms of $\{\phi_\nu\}$. The eigenfunctions $\{\phi_\nu\}$ and eigenvalues $\{\epsilon_\nu\}$ are obtained through solving the Shrödinger equation of $\hat{h}(t_j)$ similarly as the static case equation (5). Then equation (15) can be rewritten into the following form

$$\Psi_k(t_{j+1}) = \sum_\nu \langle\phi_\nu|\Psi_k(t_j)\rangle \exp[-i\epsilon_\nu\Delta t/\hbar]\phi_\nu. \tag{16}$$

Thus, the evolution of electronic wave functions and lattice configuration is determined completely by solving equations (12), (13) and (16) with a recursive trick.

3 Polaron configuration and impurities

In this section, we present the static results of a polaron in a polymer chain with an impurity. We will consider the chain consisted of 200 sites and 201 electrons in the following calculations. By the self-consistent iteration equations (5) and (7), we may first determine the polaron configuration ($\{u_n^0\}$) in the chain without any impurities. As we have said in the previous section, two kinds of impurities are considered. We discuss here their effects on the polaron configuration and binding energies.

3.1 Single-site impurity

In this subsection, we consider a single-site impurity in the polymer chain. For that,

$$V_n = V_{\rm im}\delta_{n,N_{\rm im}}, \tag{17}$$

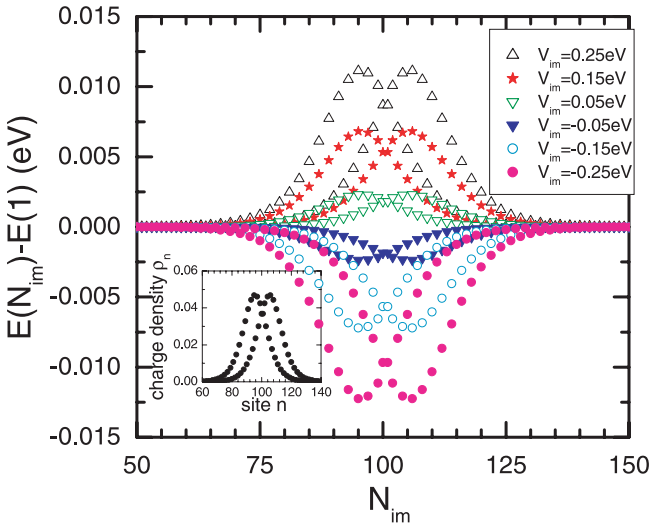

Fig. 1. Energy changement due to the presence of a single-site impurity for a fixed polaron configuration, which is obtained self-consistently in a polymer chain without any impurities. The inset shows the charge distribution of the polaron.

where $V_{\rm im}$ is the impurity strength and $N_{\rm im}$ its location. Before we present the optimized lattice configuration in the presence of an impurity, we calculation the energy changes due to the impurity at different positions for the fixed polaron configuration ($\{u_n^0\}$), which is shown in Figure 1 for the impurity strength $V_{\rm im}$ ranging from -0.25 eV to 0.25 eV. It is clear that the impurity is attractive to the negative charged polaron for the strength $V_{\rm im}$ being negative while it is repulsive for the positive impurity strength $V_{\rm im}$. An interesting thing is that the energy change reaches its maximum not for the single-site impurity locating the center of the polaron but a few sites away from the center. It will not be strange if we compare it with the charge density distribution $\rho_n(\equiv \rho_{n,n} - 1)$ of the polaron, which is shown in the inset of Figure 1.

For an attractive impurity in a polymer chain, we can do a similar calculation by using the equations (5) and (7) to obtain the optimized lattice configurations, which is a polaron binding by the impurity. In Figure 2, we show the polaron lattice configurations y_n, which is the average of bond length changes defined as

$$y_n = \frac{1}{2}(-1)^n(2u_n - u_{n+1} - u_{n-1}), \tag{18}$$

in the presence of a single-site impurity located at the 100th site. It will be not strange that the polaron deviates from the impurity since the energy change doesn't reach its maximum when the impurity locates at the polaron center as shown in Figure 1. The inset in Figure 2 shows the binding energy of the polaron, which is linear with the impurity strength at the range we consider in this paper.

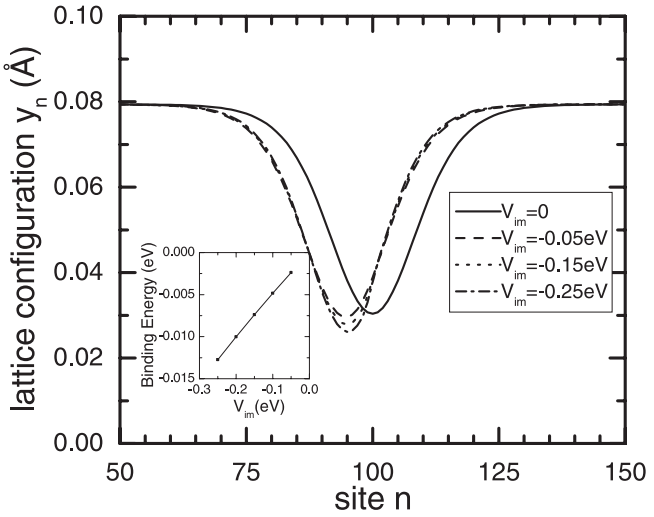

Fig. 2. Optimized polaron configurations in the presence of a single-site impurity, which is located at the 100th site. The inset shows the dependence of polaon binding energies on the impurity strength.

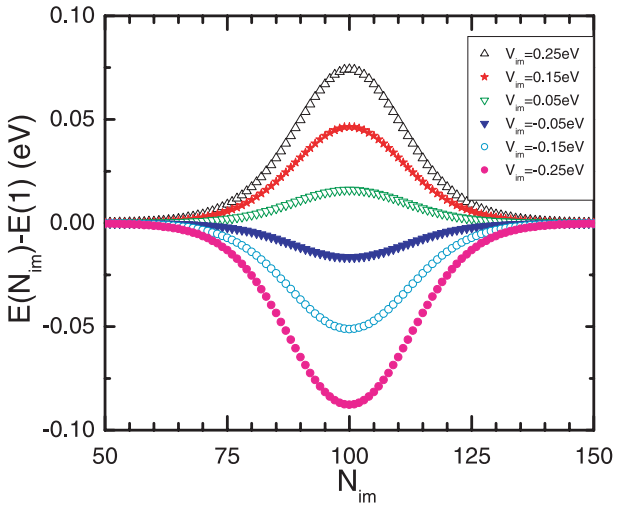

Fig. 3. Energy changement due to the presence of a multi-site impurity for a fixed polaron configuration, which is obtained self-consistently in a polymer chain without any impurities.

3.2 Multi-site impurity

The second kind of impurities we consider is defined as

$$V_n = V_{\rm im} \exp\left[-\frac{|n - N_{\rm im}|}{n_w}\right], \qquad (19)$$

which is a multi-site impurity centered in the site $N_{\rm im}$, n_w serves as the impurity width, and $V_{\rm im}$ the impurity strength as the one in the single-site impurity. In the calculation, we take $n_w = 5$, which is large enough so that the impurity makes the big difference with that of a single-site impurity, and $V_{\rm im}$ varies at the same range from -0.25 eV to 0.25 eV. In Figure 3, we show the energy change versus the location of a multi-site impurity for a fixed polaron configuration. It is clear that there is only one energy extremum point due to the multi-site impurity potential, which smears out the difference of the charge densities at these sites. The optimized polaron configurations in the presence of an attractive multi-site impurity are presented in Figure 4. The deviation of the polaron from the impurity disappears for the multi-site impurity. The inset in Figure 4 shows the binding energies for impurities with different strengths, which is again almost linear since the impurity strength is not strong.

4 Polaron depinning

In this section, we present the result of polaron depinning from an attractive impurity induced by applied electric fields. In the simulation, the impurity is set to locate at the 50th site, and the impurity strength ranges from -0.05 eV to -0.25 eV. The initial lattice configuration is the negative charged polaron that is optimized with an impurity centered at the 50th site.

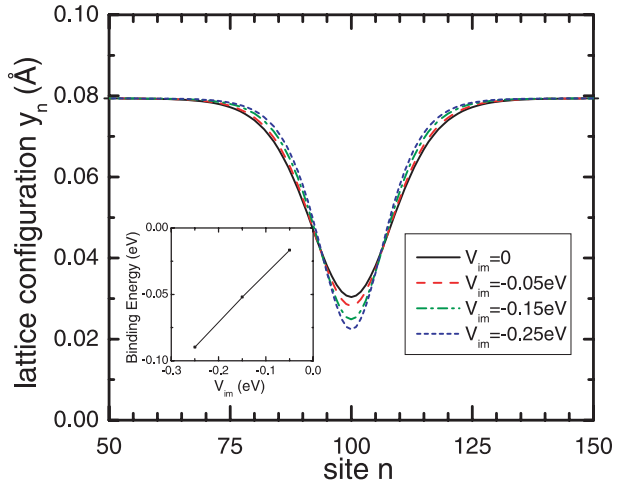

Fig. 4. Optimized polaron configurations in the presence of a multi-site impurity which is centered at the 100th site. The inset shows the dependence of polaon binding energies on the impurity strength.

In order to show the polaron motion, we define the charge center x_c of a polaron in a polymer chain with the periodic boundary condition,

$$x_c = \begin{cases} N\theta/2\pi, & \text{if } \langle\cos\theta_n\rangle \geq 0 \text{ and } \langle\sin\theta_n\rangle \geq 0; \\ N(\pi+\theta)/2\pi, & \text{if } \langle\cos\theta_n\rangle < 0; \\ N(2\pi+\theta)/2\pi, & \text{otherwise,} \end{cases} \qquad (20)$$

where

$$\theta = \arctan\frac{\langle\sin\theta_n\rangle}{\langle\cos\theta_n\rangle}, \qquad (21)$$

and the average of $\sin\theta_n$ and $\cos\theta_n$ are defined as

$$\langle\sin\theta_n\rangle = \sum_n \rho_n \sin\theta_n, \langle\cos\theta_n\rangle = \sum_n \rho_n \cos\theta_n \qquad (22)$$

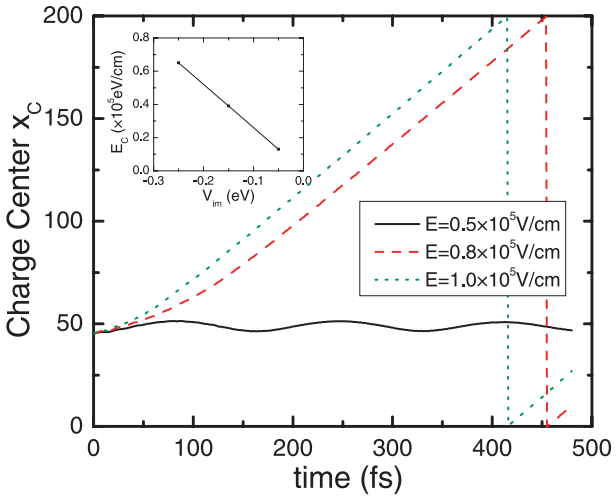

Fig. 5. Temporal evolution of the polaron charge center in the presence of a single-site impurity ($V_{\rm im} = -0.25$ eV and $N_{\rm im} = 50$) under different electric fields. The inset shows the threshold field over which the polaron depins from the impurity with different strengths.

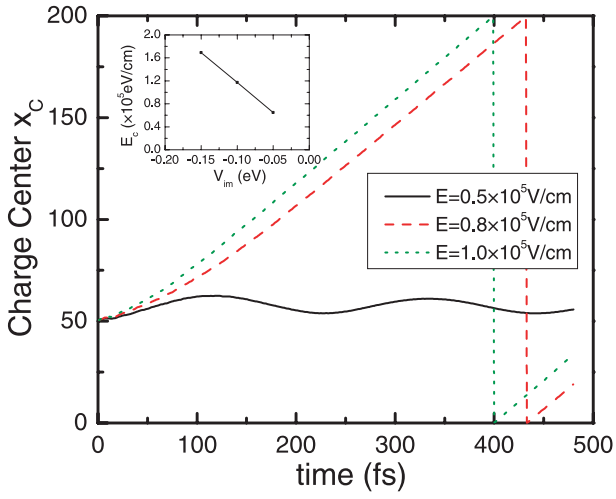

Fig. 6. Temporal evolution of the polaron charge center in the presence of a multi-site impurity ($V_{\rm im} = -0.05$ eV and $N_{\rm im} = 50$) under different electric fields. The inset shows the threshold field over which the polaron depins from the impurity with different strengths.

with the probability weight $\rho_n (\equiv \rho_{n,n} - 1)$ and $\theta_n = 2\pi n/N$, and N is the number of a polymer chain.

In Figure 5, we show the temporal evolution of the polaron charge center in the presence of a single-site impurity under different electric fields. It can be seen that there exists a threshold field, which is estimated to be 0.7×10^5 eV/cm for the impurity strength $V_{\rm im} = -0.25$ eV. The value of the threshold field is almost linear with the impurity strength (see the inset in Fig. 5). Once the applied electric filed is weaker than the threshold field, such as $E = 0.5 \times 10^5$ V/cm, the charged polaron oscillates around the impurity. A period of 168 fs is observed and the corresponding angular frequency is $0.97\omega_Q$. The oscillation amplitude is $2.4a$. However, when the applied electric filed is stronger than the threshold, the polaron will be depinned from the impurity. And then the polaron will move as the same as in a polymer chain without impurities, and a mobile multi-breather state is excited by the motion of the polaron in an electric field [10].

In Figure 6, we show the temporal evolution of the polaron charge center in the presence of a multi-site impurity. The center of this impurity $N_{\rm im}$ is set to be 50 and the impurity strength $V_{\rm im}$ is chosen to be -0.05 eV. The initial polaron is the configuration that is optimized with the multi-impurity centered at the 50th site. A similar picture is found as the case with a single-site impurity for the impurity strength is weak. For an impurity with a strong strength, for example, $V_{\rm im} - 0.25$ eV, no threshold field be found since a stronger field will dissociate the polaron [7,8]. But for the impurity strengths from $V_{\rm im} = -0.05$ eV to -0.15 eV, the threshold fields exist and showed in the inset of Figure 6, from which we can see that these values are much higher than that of the single-site impurity cases. For $E = 0.5 \times 10^5$ V/cm, the electric filed is weaker than the threshold field, the charged polaron oscillates around the impurity with a period of 214 fs, which corresponds the angular frequency $0.76\omega_Q$. The oscillation amplitude is $3.3a$. A smaller angular frequency and a lager amplitude are caused by the smoother potential of the multi-site impurity.

5 Polaron scattering

In this section, we consider the polaron scattering from an impurity, that is, the polaron is set at the place far away from the impurity at $t = 0$. In order to reduce the lattice vibration in the accelerated process of the charged polaron, the electric field is turned on and off smoothly, that is, the field strength changes as $E(t) = E\exp\left[-(t-t_c)^2/t_w^2\right]$ for $0 < t < t_c$, $E(t) = E$ for $t_c < t < t_{\rm off}$, and $E(t) = E\exp\left[-(t-t_{\rm off})^2/t_w^2\right]$ for $t > t_{\rm off}$ with t_c being a smooth turn-on period, t_w the width, and $t_{\rm off}$ the time of the filed being turned off. In the calculation, we take $t_c = 30$ fs and $t_w = 10$ fs. We have considered two processes for the polaron scattering, that is, the polaron collides with the impurity in the absence and presence of an electric field, respectively. In the former case, the electric field acts only for the acceleration of the polaron, so that the value of $t_{\rm off}$ is taken as a finite time period while it is taken as an infinite value in the latter case.

Now, we present results of the polaron scattering. In Figure 7, we show the temporal evolution of the charge center in the presence of a single-site repulsive impurity. The impurity strength $V_{\rm im} = 0.25$ eV. A negative charged polaron is set at the 50th site at $t = 0$ and the impurity is located at the 150th site. First of all, we notice that the polaron bounces against the repulsive impurity potential in the case a weak electric field, such as $E = 0.3\times10^5$ eV/cm, is applied only for the acceleration of the polaron (see the solid line in Fig. 7). However, the polaron will pass through

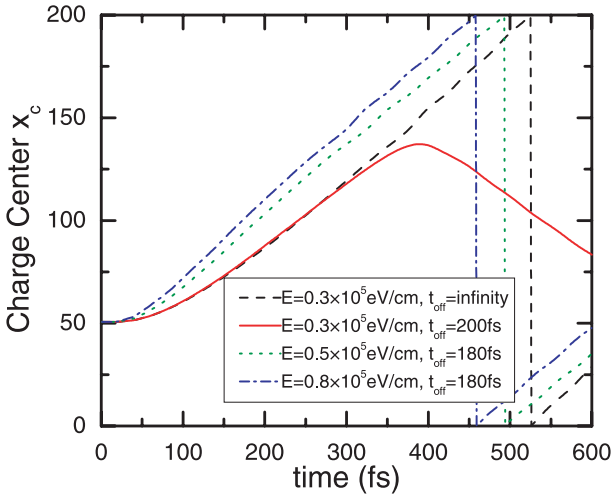

Fig. 7. Time evolution of the polaron charge center in the presence of a single-site repulsive impurity ($V_{\rm im} = 0.25$ eV and $N_{\rm im} = 150$) under the electric field with different strength.

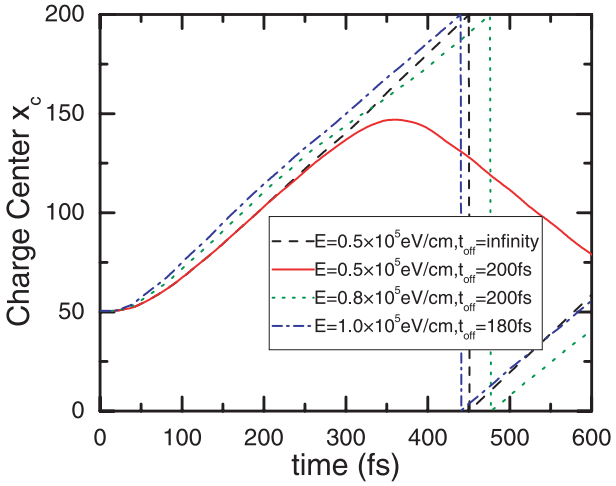

Fig. 8. Time evolution of the charge center in the presence of a multi-site repulsive impurity ($V_{\rm im} = 0.05$ eV and $N_{\rm im} = 150$) under the electric field with different strength.

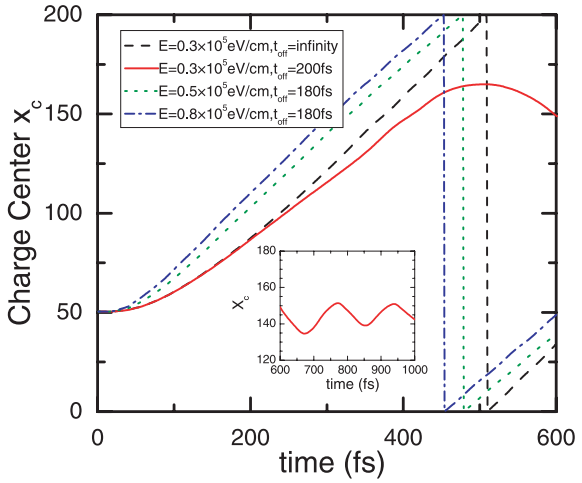

Fig. 9. Time evolution of the charge center in the presence of a single-site attractive impurity ($V_{\rm im} = -0.25$ eV and $N_{\rm im} = 150$) under the electric field with different strength.

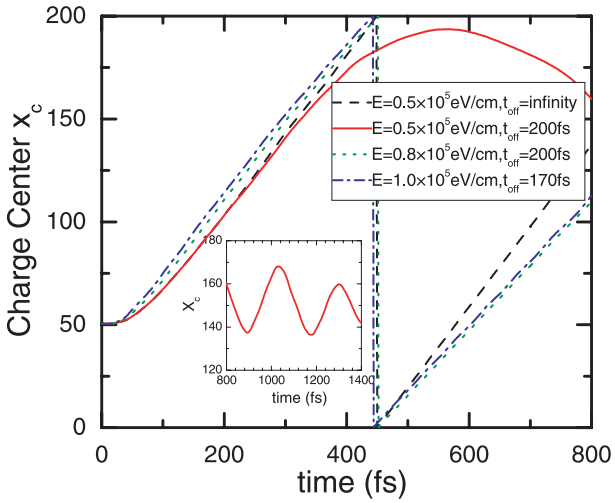

Fig. 10. Time evolution of the charge center in the presence of a multi-site attractive impurity ($V_{\rm im} = -0.05$ eV and $N_{\rm im} = 150$) under the electric field with different strength.

the impurity in the presence of the electric field (see the long dash line in Fig. 7). If the electric is higher, the polaron passes through the impurity no matter the electric field is turned off at some time or not. The critical value of the field is estimated to be 0.4×10^5 eV/cm. A similar picture is found for the polaron scattering from a multi-site repulsive impurity. We show it in Figure 8, where the impurity strength and the electric field strengths are different with that in Figure 7. For this multi-site impurity, the critical value of the field is about 0.7×10^5 eV/cm.

The situation will be different for the polaron scattering from an attractive impurity. In Figure 9, we show the temporal evolution of the charge center in the presence of a single-site attractive impurity. The impurity is located at the 150th site and the strength $V_{\rm im} = -0.25$ eV. Now the polaron will be bound by the attractive impurity in the case a weak electric field (for example, $E = 0.3 \times 10^5$ V/cm) is applied only for the acceleration of the polaron (see the solid line in Fig. 9 and that in the inset). All others are the same as that for a repulsive impurity in Figure 7. When the polaron is bound by the attractive impurity, it will oscillate around the impurity since the energy is surplus as shown in the inset of Figure 9. The oscillation period is about 177 fs, which corresponds an angler frequency of $0.92\omega_Q$. The amplitude is about $4.0a$. In Figure 10, we show the charge center evolution in the presence of a multi-site attractive impurity, the central strength of which is -0.05 eV. The critical values for attractive impurities are almost the same as that for repulsive impurities. The oscillation period is about 276 fs, which corresponds an angler frequency of $0.59\omega_Q$. The amplitude is about $12.0a$. A much smaller angular frequency and a much lager amplitude are again caused by the smoother potential of the multi-site impurity.

6 Discussion and summary

In this work, we have investigated the dynamics of a charged polaron in a polymer chain with impurities under the influence of an electric field. Two kinds of impurities, a single-site and a multi-site ones, are considered. The multi-site impurity should be more realistic in polymers. The results for these two kinds of impurities are found qualitatively same. As is well known, the polaron will be dissociated by a stronger field [7–9]. For this reason, we only consider the electric fields with strengths between 0.1×10^5 eV/cm and 2.0×10^5 eV/cm, (a smaller electric field is not considered since it will take too much CPU time in the calculations) and then the impurity strengths are chosen between ± 0.25 eV. As usual, the electron-electron interaction is thought to be not negligible. Actually, it is really a challenge to include the electronic correlation in a dynamical study while no qualitative difference be found if the interaction is treated only within a mean-field approximation, that is the reason why we don't include the interaction in this work. In reference [14], the impurity molecules were considered to function as logical switches and polarons (as well as bipolarons) are used as information carriers, so that the impurity molecule can work as a gate to the passage of charged polarons or bipolarons, i.e., it can control the charge transport. Our study points out that the polaron is trapped by the attractive impurity only for the case a weak electric field is presented for the acceleration of the polaron while the polaron will pass through the impurity in the case the same electric field is kept on. The result is also consistent with that the pinned polaron will be dragged away by a relative stronger electric field. In the other hand, we also consider the polaron scattering from a repulsive impurity. A new picture that the polaron may bounce against the repulsive impurity is found in the same condition for the polaron being trapped by the attractive impurity. In the sense, this work offers a complete picture for the dynamics of a polaron in a polymer chain with impurities.

In summary, we simulate the dynamical process of polaron in a polymer chain with impurities within a non-adiabatic evolution method, in which the electron wave function is described by the time-dependent Schrödinger equation while the the polymer lattice is treated classically by a Newtonian equation of motion. We have considered two kinds of dynamical processes, one is the field-induced depinning of a charged polaron, which is initially bound by an attractive impurity; and the other is the scattering of a polaron from an impurity. In the former process, the charged polaron will depart from the attractive impurity only for the applied field with strength over a threshold, otherwise, the polaron will oscillate around the impurity. In the latter process, the charged polaron moves through the impurity in the presence of an electric field while it will be bounced back for a repulsive impurity or trapped to oscillate around an attractive impurity in the case that the applied electric field is weak and just be present for the polaron acceleration.

This work was partially supported by National Natural Science Foundation of China (Grant Nos. 90103034, 10204005, 10374017, and 10321003) and the State Ministry of Education of China (No. 20020246006).

References

1. I.H. Campbell, D.L. Smith, Solid State Physics **55**, 1 (2001) and references therein
2. W.P. Su, J.R. Schrieffer, A.J. Heeger, Phys. Rev. Lett. **42**, 1698 (1979)
3. S.A. Brazovskii, N.N. Kirova, Sov. Phys. JETP Lett. **33**, 4 (1981)
4. A.J. Heeger, S. Kivelson, J.R. Schrieffer, W.P. Su, Rev. Mod. Phys. **60**, 781 (1988)
5. W.P. Su, J.R. Schrieffer, Proc. Natl. Acad. Sci. USA **77**, 1839 (1980)
6. Y. Ono, A. Terai, J. Phys. Soc. Jpn **59**, 2893 (1990)
7. S.V. Rakhmanova, E.M. Conwell, Appl. Phys. Lett. **75**, 1518 (1999)
8. A. Johansson, S. Stafström, Phys. Rev. Lett. **86**, 3602 (2001)
9. C.Q. Wu, Y. Qiu, Z. An, K. Nasu, Phys. Rev. B **68**, 125416 (2003)
10. J.F. Yu, C.Q. Wu, X. Sun, K. Nasu, Phys. Rev. B **70**, 064303 (2004)
11. A.R. Bishop, D.K. Campbell, P.S. Lomdahl, B. Horovitz, S.R. Phillpot, Phys. Rev. Lett. **52**, 671 (1984); A.R. Bishop, D.K. Campbell, P.S. Lomdahl, B. Horovitz, S.R. Phillpot, Synth. Met. **9**, 223 (1984)
12. S.V. Rakhmanova, E.C. Conwell, Synth. Met. **110**, 37 (2000)
13. A. Terai, Y. Ono, J. Phys. Soc. Jpn **60**, 196 (1991)
14. C. da S. Pinheiro, G.M. e Silva, Phys. Rev. B **65**, 094304 (2002)